Battery Pack Design and Thermal Management System for Formula Student Electric Race Car

Yash Kulkarrni[1, a], Vinayak Chougule[1, b], Ankur Harge[1, c], Shantanu Kumbhar[1, d], Prachi Gadekar[1, e], Sagar Kadam[2, f]

Author Affiliations

[1]*Mechanical Engineering, College of Engineering Pune, 411005 India*
[2]*Associate Professor, Dept. of Mechanical Engineering, College of Engineering Pune, 411005 India*

Author Emails

[a)] yashyk1999@gmail.com
[b)] veenayakdc@gmail.com
[c)] hargeankur@gmail.com
[d)] shantanukumbhar12@gmail.com
[e)] impulseprachi679@gmail.com
[f)] smk.mech@coep.ac.in

Abstract. Formula Student (FS) Competition provides a platform for engineering students to showcase their ability to conceptualize, design and produce a working model of a formula style race car. With aim to tackle growing concerns of fossil fuel stock, environmental impact and climate change, governments around the world are embracing new technologies. One such technology being electric vehicles (EV). In light of this push to move away from fossil fuels and to embrace electric technology, the host organization has put together a series of initiatives under the Formula Student banner to build a platform for students interested in switching to the Formula Student Electric category. But EVs is still in its nascent stage of development; and thus, the field is highly esoteric from student's point of view. Accumulator is one of the most important parts of an electric race car; it powers the entire car along with its tractive system. The paper demonstrates a simple approach at achieving a suitable battery design and its thermal management. Beginning with selection of suitable motor for drivetrain followed by estimation of energy requirement through MATLAB OpenLap simulation. Basis this requirement, a suitable cell configuration is designed. The battery pack is a potential source of heat generation and for its optimal performance during the race day, thermal management system is of utmost importance. A fan-based cooling system is devised to handle this heat load. This approach though not too complex provides a comprehensive method, right from motor selection to thermal system design for Formula Student racecar.

Keywords: Accumulator, battery pack, cell chemistry.

1. INTRODUCTION

While shifting gears from combustion to electric powertrain can be challenging for the freshers, main challenge that these teams face is during accumulator design process. Accumulator system involves battery pack which are composed of several segments; these are united through a single data bus that enables segments control using battery management system (BMS). Electronic control Unit (ECU) is also connected to the data bus. It processes the data and controls the traction motor controllers. Accumulator Isolation Relays serve to breaking the electric circuit of pack in

the case of crash, short circuit, overheating and other emergencies. These are basically high-voltage (HV) contactors which are used as a switch to enable high voltage on the vehicle when vehicle is in ready to drive condition. When AIRs are turned on, HV is supplied from battery pack to Motor controllers through relays. These are operated on 12V supply. 3 contactors are used in total - One for HV+, second for HV- and last one for recharge circuitry. Given the significance, it is very important not to under design or over-design a battery pack. Plus, care needs to be taken to remain within the bounds of design and safety regulations of the competition. Designing can include selection of cells, simulations, testing and validation of battery pack. But the process begins with selection of a suitable motor for your tractive system. The propulsion calculation [1] gives us the necessary peak power and torque requirement. This will give us important feedback in terms of specification required for the motor. Once the motor is selected, energy requirement becomes essential next step to determine the battery characteristics. C.Hariharan, et al demonstrated how MATLAB simulation can be used to develop transient simulation model. It facilitated to take into account variations such as driving condition, altitude, orientation, ambient temperature while calculating the remaining driving range. In some case [3] a nonlinear regressive approach gives better estimate of the drive range through energy calculation. But this approach is complex compared to traditional model-based approach with only slight improvement in the estimates.

Cell chemistry involves study of different cell structure and composition to choose a suitable cell for a given application. At present, lithium-ion cells are widely adopted in electric vehicles (EVs) and hybrid electric vehicles (HEVs) for such advantages as high- power density, low self-discharge ratio, low maintenance, large output power and high open circuit voltage [4]. There are several literatures that offer large number of Li-ion battery models which focus on different aspects of battery namely electric, thermal, and aging [5]. In the literature, lifetime estimation of Li-ion batteries is performed in the laboratory, often with accelerated tests, where battery stress factors and levels are chosen to accelerate the desired aging phenomenon [6,7]. From these measurements semi-empirical models have been derived [8]: the most discussed ones are based on lithium nickel cobalt aluminum (NCA), lithium iron phosphate (LFP) chemistries [9] and lithium manganese oxide–nickel manganese cobalt chemistry (LMO-NMC) [10,11].

Nevertheless, the heat generation of the lithium-ion cell greatly increases upon the surges of charge and discharge ratio [12]. The working temperature has a large impact on the electrochemical properties of the lithium-ion cell [13]. When the working temperature exceeds 323.15 K, the decomposition reaction of the electrolyte, the degradation of the cathode, and the growth of the solid electrolyte interface (SEI) membrane are accelerated, which cause decrease of battery performance and the reduction of discharge capacity [14,15]. To confine the optimized operating temperature of lithium-ion cell in range of 20–50 ◦C and the highest temperature difference lower than 5 ◦C [16,17], it is vital to design an effective battery thermal management system (BTMS). Though liquid cooling has become a mainstream method in BTMS because of its high heat dissipation efficiency [18] same would not be feasible in case of a student race car given the time and space constraints.

Though the literatures provide a segmented solution to individual problems, a holistic approach which could capture all the steps at once is missing. Given these considerations, a complete approach, right from motor selection to thermal system design was desirable. And same is demonstrated step-by-step through this paper.

- Nomenclature

M_a	Mass of Equipped Car (*kg)*
g	Acceleration due to gravity *(m/s^2)*
f_k	Coefficient of rolling resistance of a strained wheel on unstrained surface
f_0	Friction factor for smooth asphalt
A_f	Coefficient of efficiency of speed on rolling resistance *(s^2/m^2)*
V_{max}	Specified max speed of car *(m/s)*
c_x	Car drag coefficient
ρ_{air}	Air density (kg/m^3)
A	Car mid-length cross-section area (m^2)
n_{tr}	Coefficient of efficiency of transmission system
K_p	Electric power operation factor
Nu	Nusselt Number
Re	Reynolds Number
Pr	Prandtl Number *(m^2/s)*

2. MODEL IMPLEMENTATION

2.1 Motor Selection

The first stage of accumulator design processes - most important for any electric race car - is to select a suitable motor. Acceleration event at Formula Bharat checks for the minimum time required to cover a 70m of straight patch on the circuit. Thus, a motor should provide the required propulsion in sufficiently less time so that it meets the acceleration target of the team. Plus, many other factors are to be considered while selecting an optimal motor such as what is the maximum and continuous torque requirement, top speed requirement, cost, motor type and others. Thus, to get the requirements for the torque and peak motor power, we have performed propulsion calculations via A.Sh.Khusainov's procedure.

$$P = \frac{M_a.g.f_k V_{max} + 0.5 c_x.\rho_{air}.A.V_{max}^3}{\eta_{tr} K_p} \quad \text{…. (1)}$$

Where, $f_k = f_0\left(1 + A_f.V_{max}^2\right)$

The peak power calculated out of this formula was 28 KW. Plus, maximum torque characteristics of the selected motor should supplant the peak torque requirement condition. Force balance equation facilitates to get a rough estimate of this torque requirement.

$$F_{tr} = F_{roll} + F_{up} + F_{air} + F_{in} \quad \text{….. (2)}$$

Where,

$F_{tr} = \frac{\eta_{tr}.M.i_0.i_1}{r}$ $is\ tractive\ force$; $M\ is\ torque\ on\ motor\ shaft$;

$i_1\ and\ i_0\ is\ the\ gear\ ratio\ of\ main\ gear\ and\ first\ gear$; $r\ is\ the\ wheel\ radius = 0.25m$

$F_{roll} = f_k.m.g.\cos(\alpha) - rolling\ friction\ force$; $\alpha\ is\ the\ inclination\ angle = 0°$

$F_{up} = m.g.\sin(\alpha) - resistance\ force\ due\ to\ gravity$

$F_{air} = (0.5)c_x.\rho_{air}.A.V_{max}^2 - force\ of\ air\ resistance$

$F_{in} = \text{m.a.}\sigma_r - inertial\ force$; $\sigma_r\ compensation\ factor\ for\ rotating\ mass$

Thus, the peak torque for electric motor is given as,

$$M = \frac{\left(f_k.m.g.\cos(\alpha) + m.g.\sin(\alpha) + 0.5.c_x\rho_{air}.A.V_{max}^2 + m.a.\sigma_r\right).r}{\eta_{tr} i_0 i_1} \quad \text{…. (3)}$$

For our car the i_1 main gear ratio was 1, while the first gear ratio which depends upon the motor was derived through iteration method at various operating motor speeds.

TABLE 1. Peak motor torque iteration

i_0	ω	M_{peak}	i_0	ω	M_{peak}
1	111.08	608.3124	3.5	388.78	173.8035
1.5	166.62	405.5416	4	444.32	152.0781
2	222.16	304.1562	4.5	499.86	135.1805
2.5	277.7	243.325	5	555.4	121.6625
3	333.24	202.7708	5.5	610.94	110.6023

Considering above results for the peak torque and power requirement, we found that high efficiency and low weight of HPEVS AC 23 makes it a certain pick for our purpose. These types of motors are highly efficient in producing a large amount of torque over a vast speed range. The characteristics of torque delivery from motor match with the demands of the powertrain neatly.

TABLE 2. HPEVS AC 23 Motor specifications

Parameter	Specification
Operating Voltage	72 V
Nominal Current	140 Amps
Peak Current	522.8 Amps
Peak Torque	143.4 Nm
Continuous Torque	19 Nm
Peak Power	32 KW
Continuous Power	12 KW
Gear Ratio i_0	4.5
Cooling	Forced Air cooling with Fan
Weight	27.2 Kgs
Manufacturer	USA

2.2 Energy Requirement Calculations

After the selection of optimal motor, the next phase was to calculate the energy requirement. For this calculation we have taken into account the event for which maximum amount of energy would be required. And the event is the Endurance test. This test demands the car to perform for continuous 22 laps i.e approx. 22 km in a single charge. Based on the motor selected and considering the track data we have simulated our car's model in OpenLap, an open-source software in MATLAB. All the vehicle dynamic and aero parameters were taken into consideration which includes motor torque curve, drivetrain, tires, aerodynamics, and steering models. Also, track was generated from segments or logged data.

TABLE 3. Vehicle Setup Chart

Category	Description	Value	Unit	Comment
Inertia	Total Mass	250	kg	
	Front Mass Distribution	45	%	
Dimensions	Wheelbase	1620	mm	
Steering	Steering Rack Ratio	5		[Steering Wheel Angle]/Wheel Angle]
Aerodynamics	Lift Coefficient CL	-1.5		Positive = Lift / Negative - Downforce
	Drag Coefficient CD	-0.8		Should be negative
	CL Scale Multiplier	1		
	CD Scale Multiplier	1		
	Front Aero Distribution	50	%	
	Frontal Area	1.3	m2	
	Air Density	1.225	kg/m3	Recommended value: 1.225
Brakes	Disc Outer Diameter	185	mm	Assumed to be the same on all corners.
	Pad Height	76	mm	Assumed to be the same on all corners.
	Pad Friction Coefficient	0.35		Assumed to be the same on all pads. Recommended value: 0.45
	Caliper Number of Pistons	3		Assumed to be the same on all corners.
	Caliper Piston Diameter	31.75	mm	Assumed to be the same on all corners.

	Master Cylinder Piston Diameter	16.02	mm	Assumed to be the same both front and rear.
	Pedal Ratio	4.68		[Foot Force Application Point Lever Arm]/[Master Cylinder Lever Arm]
Tyres	Grip Factor Multiplier	1		
	Tyre Radius	203	mm	Assumed to be the same on all tyres.
	Rolling Resistance	-0.001		Assumed to be the same on all tyres. Needs to be negative. Recommended value: -0.001
	Longitudinal Friction Coefficient	1.5		Assumed to be the same on all tyres. Slick tyres: 1.8, Street tyres: 0.9-1.2
	Longitudinal Friction Load Rating	75	kg	Assumed to be the same on all tyres. Recommended value: M/4
	Longitudinal Friction Sensitivity	0.0001	1/N	Assumed to be the same on all tyres. Should be positive. Recommended value: 0.0001
	Lateral Friction Coefficient	1.4		Assumed to be the same on all tyres. Slick tyres: 1.8, Street tyres: 0.9-1.2
	Lateral Friction Load Rating	75	kg	Assumed to be the same on all tyres. Recommended value: M/4
	Lateral Friction Sensitivity	0.0001	1/N	Assumed to be the same on all tyres. Should be positive. Recommended value: 0.0001
	Front Cornering Stiffness	450	N/deg	Recommended value: 800-1000
	Rear Cornering Stiffness	551	N/deg	Recommended value: 800-1000
Engine	Power Factor Multiplier	1		
	Thermal Efficiency	0.3		Recommended value: 0.3 for ICE
	Fuel Lower Heating Value	4.72E+07	J/kg	Recommended value: 4.72E+07 for petrol
Transmission	Drive Type	RWD		
	Gear Shift Time	0.01	5	Only used in dragster mode
	Primary Gear Efficiency	0.98		Recommended value: 0.98 for spur/helical gears
	Final Gear Efficiency	0.98		Recommended value: 0.90 for bevel gears
	Gearbox Efficiency	0.98		Recommended value: 0.98 for spur/helical gears
	Primary Gear Reduction	1		From crankshaft to Input shaft.
	Final Gear Reduction	5.31		
	1st Gear Ratio	1	-	
	2nd Gear Ratio		-	
	3rd Gear Ratio		-	

After the input data file was uploaded, we needed to upload the motor characteristic curve data which consisted of speed vs power curve, traction curve and the gearing curve. Motor curve of the selected motor shows that the peak power of 32KW i.e approx. 42 Hp was obtained at close to 2700 rpm. Motor tractive force was limited by final tractive force in order to avoid any slip which can result due to excess tractive force generated by the motor.

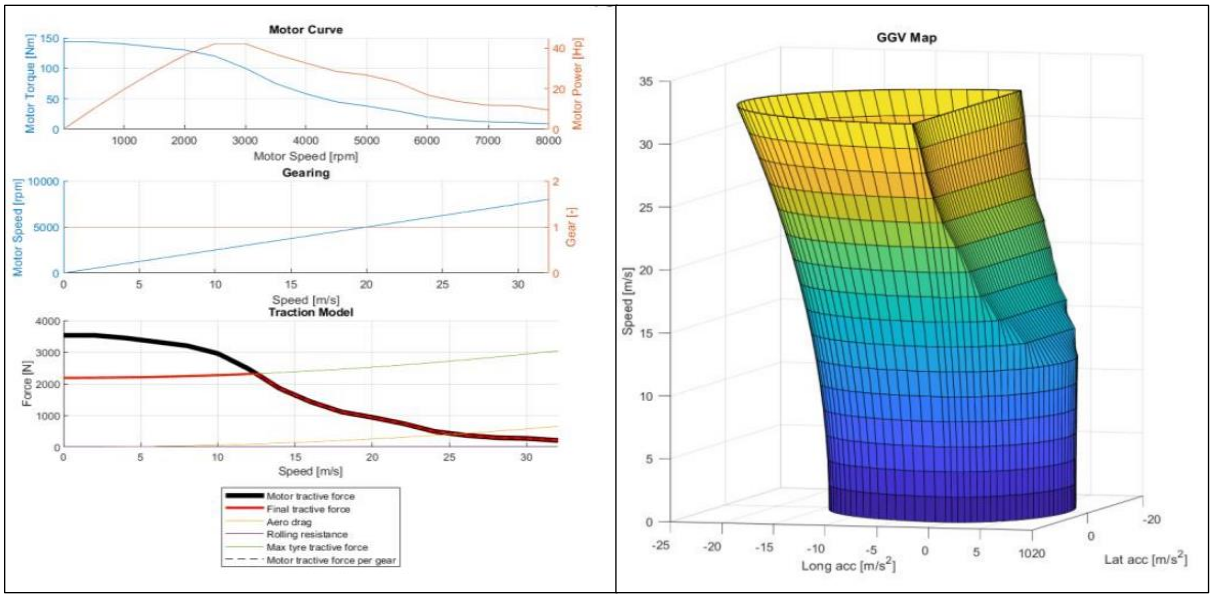

FIGURE 1. Open Lap Vehicle Model

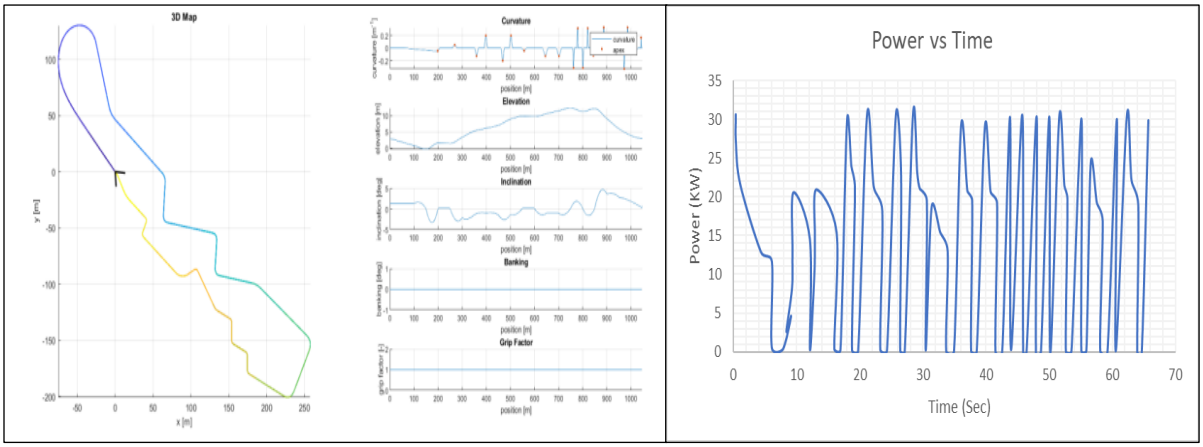

(a) (b)

FIGURE 2. a) Formula Bharat Track Generation file using Open Track. b) Simulation results

From the simulation results, logged data of motor power vs time was plotted and area under the curve was calculated using numerical methods which gave us the energy requirement for 1 Lap of track. Hence multiplying it to get the requirement for 22 Laps we get the **Total Accumulator Peak Energy** requirement. However, considering safety factor we have considered 6.2 kWh for designing accumulator.

TABLE 4. Energy Requirement

1 Lap Distance	1046 m
1 Lap Energy Requirement	0.26 kWh
Total Accumulator Requirement	5.62 kWh

2.3 Cell Selection

- **Cell Chemistry selection**

Ragone plots were referred initially for cell selection. These plots are basically used to compare the performance of various energy storing elements. The chart is basically plotted for comparison of specific energy v/s specific power. Specific energy determines the total amount of charge that can be released from the element and specific power determines the rate at which the charges can be released from the element.

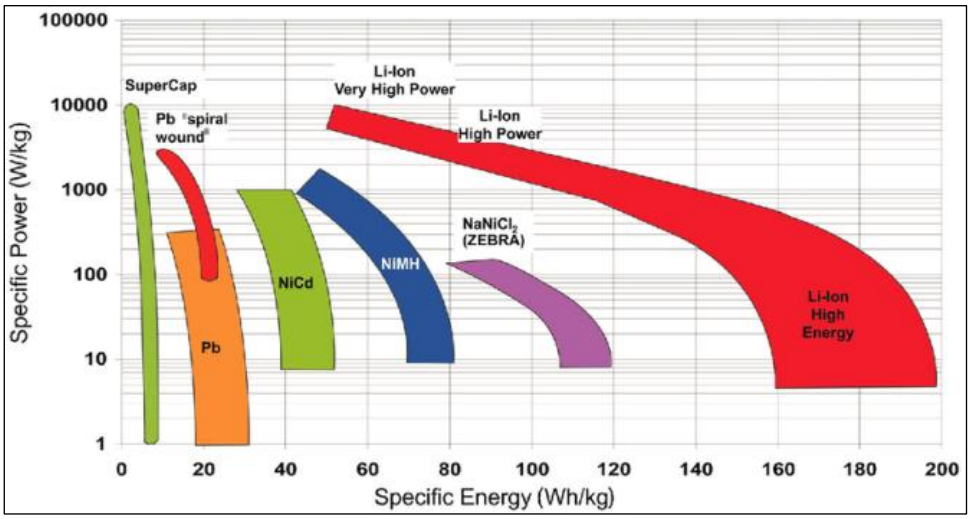

FIGURE 3. Ragone Plots

As seen from the Ragone plot, Li-ion cells have high specific energy and sufficient specific power, where as other cell chemistries and super capacitors do not have much storage capacity. Based on this plot, further different li-ion chemistry cells were compared to select safe and efficient cells. Parameters that were considered for comparison were specific energy (Wh/kg), Nominal Voltage(V), Charge Rate(C), Discharge Rate(C) and Thermal Runaway(˚C).

TABLE 5. Comparison of Cell Chemistry

Parameters	**LiFePo4**	**NMC**	**LiCoO2**	**LMO**	**NCA**	**LTO**
Nominal Voltage(V),	3.2	3.7	3.6	3.7	3.6	2.4
Specific Energy (Wh/kg),	90-120	150-220	150-200	100-150	200-260	50-80
Charge Rate(C)	1	0.7-1	0.7-1	0.7-1	0.7	1
Discharge Rate(C)	1	1	1	1	1	1
Thermal Runaway(˚C)	270	210	150	250	150	Safest

Based on the above comparison between different li-ion chemistries it was found that Nickel Magnesium Cobalt oxide chemistry were more suitable to our design. NMC cells which have 3.7-volt nominal voltage will be useful in reducing the number of cells to be connected in series and a nominal specific energy which would ensure a smaller number of cells to be connected in parallel.

- Cell geometry and manufacturer selection

Lithium-ion cells are available in different shapes such as cylindrical, pouch and prismatic as well as different manufacturer brands. So, it was necessary to finalize the shape of the cells before starting the design of the battery pack. The different parameters considered while cell shape selection was: Cost and Weight, Ahr Capacity, Packaging Efficiency. Based on this comparison, we decided to choose Li-Ion NMC chemistry pouch cell for designing our high

voltage battery pack as their weight and cost are medium and also have sufficient Ahr capacity, to satisfy our needs. To ensure optimal performance from the accumulator, a significant amount of time was devoted towards extensively investigating as many battery cells options as possible. Both packaging criteria and performance data was considered. And after comparing a number of NMC cells from different cell manufacturers, and from the other constraints considered, like availability, lead time and cost **SLPBA390190** cell was selected from **Melasta** for designing of our high voltage battery pack.

TABLE 6. Cell Parameters

Parameters	Values
Nominal Cell Voltage	3.7V
Maximum Cell Voltage	4.2
Minimum Cell Voltage	3.0V
Ahr Capacity	21Ahr
Maximum Peak Output Current	420A(≤3Sec)
Maximum Nominal Output Current	210A
Charging Current	10A
Maximum Cell Temperature (Discharging)	60˚C
Maximum Cell Temperature (Charging)	45˚C
Weight	0.409kg

2.4 Accumulator configuration

The total number of cells required for designing the required high voltage battery pack is determined on the basis of the motor parameters and total power required for completing Endurance test. Based on the power required, the total capacity of the battery pack is determined. Considering the motor controller and motor operating voltage(72V), no. of cells to be connected in series are determined. Further, basis the voltage and capacity, Ahr capacity of the battery pack is determined. From previous Open lap simulation, 6.2kWh, capacity was considered for designing the battery pack. Analyzing all these parameters and accounting for the Formula Student rules a 72V,84Ahr system was decided to build.

The total number of cells to be connected in series is determined from the required nominal voltage of the battery pack and nominal voltage of each cell.

$$Nominal\ Voltage\ of\ battery\ pack = Nominal\ voltage\ of\ cell\ \times No.of\ cells\ in\ series \quad \ldots.(4)$$

$$72V = 3.7 \times No.\ of\ cells\ in\ series$$

No. of cells in series = 20;

Further we can calculate the number of cells to be connected in parallel to achieve the require Ahr capacity from the total Ahr capacity of the battery pack and Ahr capacity of each cell.

$$Ahr\ capacity\ of\ battery\ pack = Ahr\ capacity\ of\ single\ cell\ \times No.of\ cells\ in\ parallel \quad \ldots.(5)$$

$$84 = 21 \times No.\ of\ cells\ in\ parallel$$

No. of cells in parallel = 4;

Thus, a 20s4p battery pack was considered for design of accumulator. These cells needed to be arranged in the form of segments. Each segment was limited by rules to have mass ≤ 12 kg, energy ≤ 6MJ and static voltage ≤ 120VDC. Iterating process was carried to get the most optimal configuration. In 1st as well as 4th iteration, the maximum energy of the segment is going above 6MJ, in so this type of segment distribution is rejected. While 3rd iteration doesn't violate any parameters, it would be difficult to design a symmetrical battery pack and to ensure uniform weight

distribution. Further due to nominal voltage of both the segments would be less than 12V, it would be difficult to calibrate BMS for individual segment, and so this design was discarded. 5 segment 4s4p configuration was selected for accumulator design.

TABLE 7. Segment configuration iteration

Parameter	Segment configuration			
	4 segments of 5s4p	5 segments of 4s4p	6 segments of 3s4p and 1 segment of 2s4p	4 segments of 20s1p
Maximum Static Voltage	21V	16.8V	12.6V	8.4V
Ahr Capacity	84Ahr	84Ahr	84Ahr	84Ahr
No. of cells/segment	20	16	12	8
Maximum Energy	6.35MJ	5.08MJ	3.81MJ	2.54MJ
Estimated Weight	8.18kg	6.544kg	4.908kg	3.272kg

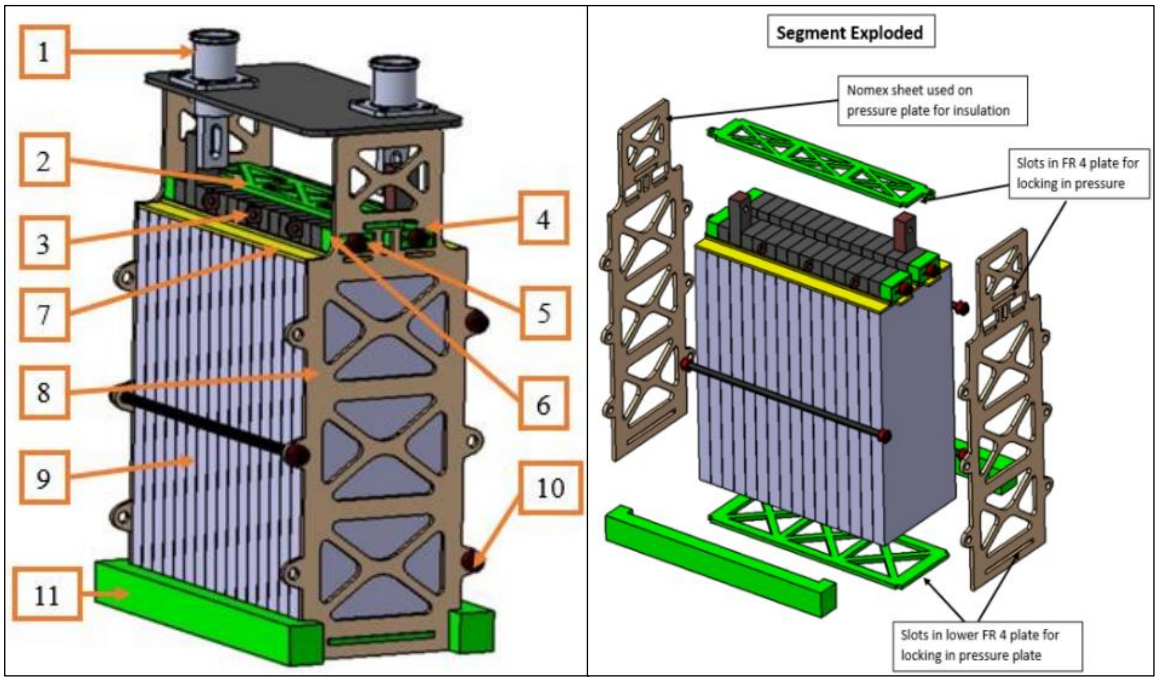

FIGURE 4. Segment details and Exploded view

Considering the vibration and dynamic impact, the assembly is designed. The cells are placed between the pressure plates (8) and the series parallel combinations are made by using FR4(2) and aluminum (3) busbars. The whole segment assembly is bolted to the container using metal studs (5) to avoid horizontal and vertical position. Aluminum busbars and the cell tabs (9) are center drilled through which a hallow glass fiber bush (4) is passed completely throughout the cells and busbars, a metal stud (5) is then passed through the hallow glass fiber bush and is positively locked at both the ends. The lower FR4 plate (7)(plate below busbar) is press fitted in the side pressure plates(8) . Also, to ensure proper insulation between segment and container wall Nomex paper is pasted to the walls using Nomex tape. The segments have a FR4 insulation plate at top to avoid any direct with the cells, if by chance any tool falls on the segment while working on it. These segments are further rested between FR4 blocks (11). The output is drawn through receptacle (1) which connect other segments in configuration. The overall arrangement of entire accumulator is shown in Fig 5.

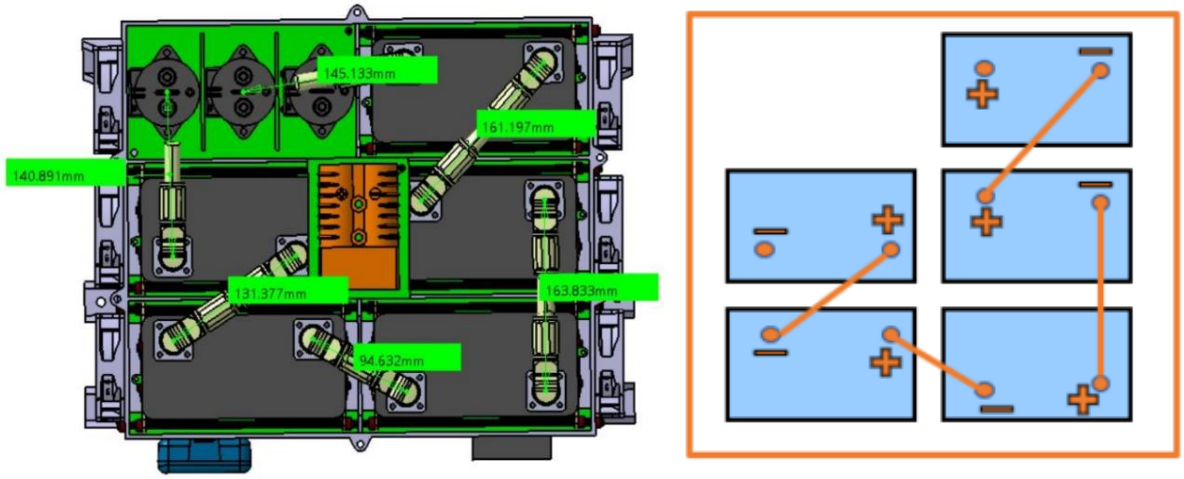

FIGURE 5. Maintenance Plugs Connection and segment polarity

2.5 Thermal management of battery

One of the reasons, for heat dissipation in battery is due to I^2R losses taking place in battery due to internal reactions taking place inside the cell, and due to I^2R losses due to internal resistance. The other sources involve, busbar contact resistance. So, in-order to reduce the heat dissipation inside the battery, it is very essential to design busbar, which can not only reduce the contact resistance but also facilitate sufficient cooling of the cell tabs. Positive locking of the bush bars using studs reduces the effect of contact resistance to a large extent. So certain assumptions were considered while designing the thermal management system. Heat generated as a result of internal cell reaction and contact resistance is considered to be negligibly small relative to the cell's internal resistance. The battery characteristics suggest that a single segment dissipates to a maximum of 302.5W. And accumulator configuration with 2 segments in each row suggest a total heat dissipation of 605W per row.

TABLE 8. Segment configuration iteration

Segment configuration	4S4P
Cell Internal DC Resistance	1mΩ
Peak cell current	137.5A
Max heat dissipation (1 Cell)(I^2R)	18.91W
Max heat dissipation (4P module)	75.63W
Max heat dissipation (1 Segment)	302.5W
Max heat dissipation (1 row i.e 2 segments)	605W

In order to remove the dissipated heat, forced convective air cooling via a fan was carried. Desired final temperature was 35˚C temperature and initial and final temperature of air was taken as 25 ˚C and 45 ˚C respectively. Thus, given the heat dissipation, we can calculate the convective heat transfer coefficient; which in our case turn out to be 466.86 W/m^2K. Hence, we get the Nusselt number as 7469.79. Knowing these values coupled with some other properties of air (at 35˚C) we get the required CFM of the fan

Consider the below equation for the condition of combined laminar and turbulent flow:

$$Nu = (Re^{0.8} - 23200) \times (0.0375)Pr^{1/3} \quad \text{..... (6)}$$

Thus,

$$Re = 54.43 \times 10^5$$

Required airflow at fan inlet,

$$Mass\ flow\ rate = Area \times Velocity$$

$$Mass\ flow\ rate = 0.002025 \times 21.92\ m^3/s$$

$$Mass\ flow\ rate = 0.04439\ m^3/s\ \ i.e\ \ 94cfm$$

Total mass flow rate required to remove heat generated by forced air convection method is 94cfm. Depending upon the system pressure drop we have to finalize the fan which can overcome all the pressure drop generated in the system due to friction, convergence, divergence of flow tunnels. There are 3 sources contributing to system pressure drop which includes loss from sides, holes and loss from Darcy-Weisbach equation. Loss through holes is calculated using Zigrang-Sylvester equation for flow through pipe.

TABLE 9. System and Fan pressure drop condition

Flow Rate (cfm)	System pressure drop	Single fan pressure drops	Series fan pressure drop
1	0.001223672	13	26
10	0.096689498	12	24
20	0.376375913	10.5	21
30	0.838274839	9	18
40	0.482329062	7.2	14.4
50	0.308523684	6	12
60	3.316853034	5.5	11
70	4.507314456	5	10
80	5.879906521	4	8
90	7.434628383	2.7	5.4
100	9.171479506	0	0

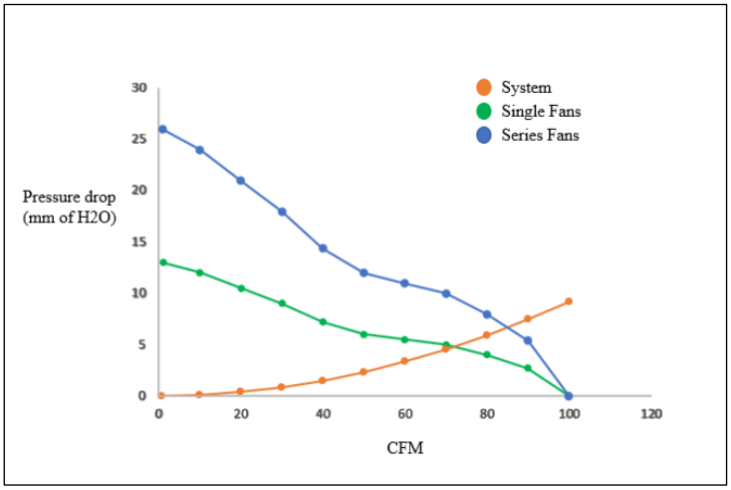

FIGURE 6. Pressure Drop Graph

With single fan cooling arrangement, it is evident that system pressure drop crosses fan pressure drop at approx. 70 cfm. Beyond 70 cfm, system drop is dominating and exceeds the pressure drop generated by the fan. Due to this single fan would fail to provide adequate cooling which demands for 94 cfm. In order to resolve the issue a series fan configuration is employed. The graph shows that intersection point is pushed close to 90 cfm thus providing an adequate output to overcome the system drop. We performed ANSYS CFD analysis for simulating

real life thermal conditions of one battery segment. We compared the thermal results for 3 different designs of cell tabs with variable hole sizes and locations to finalize the cell busbar design. Input Parameters were: 1. Heat dissipation in terms of W/m^3 2. Inlet air velocity of 11m/s as a boundary condition 3. Inlet air temperature of 25 ℃ as a boundary condition.

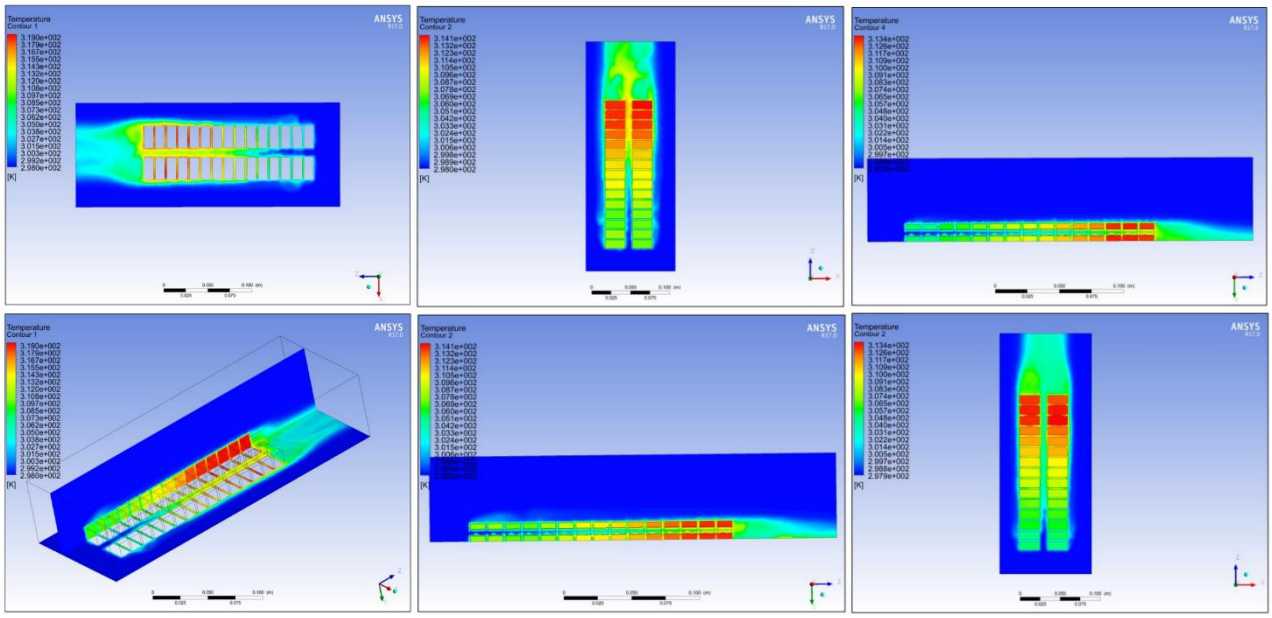

(a) (b) (c)

FIGURE 2. a) Solid busbar with no holes b) Bushbars with 1 hole of 6mm c) Bushbars with 2 holes of 4mm

Comparing the above 3 designs on the basis of temperature contours generated along the segment length, it can be concluded that Iteration 3 is best suited for our application with highest uniform temperature distribution profile and minimum peak temperature.

TABLE 10. Maximum temperature for different busbar designs

Design	Maximum temperature
Solid Busbars	319K
Busbars with 1 hole of 6mm	314.1K
Busbars with 2 holes of 4mm each	313.4K

CONCLUSION

Through this article we discussed a methodology-cum-approach to give a holistic solution for designing a suitable battery pack for the Formula student race car. This methodology consisted of five steps. The first step was to calculate the motor characteristic specification requirement which included peak power and torque requirement. Basis brushless HPEVS AC 23 was selected. The second was OpenLap simulation in MATLAB to get the estimate of the energy requirement. In this, the input provided for the simulation took into account all the parameters right from motor characteristics, friction, aerodynamics to track layout. This couple with safety factor gave us the battery energy requirement. The next step involved cell chemistry to select a suitable cell. We discussed about the thought that went into selecting **Melasta SLPBA390190** cell. Fourth step which followed was to choose a suitable segment configuration as per the Formula Student rules and get the optimum arrangement. Finally, thermal calculation us the CFM requirement for fan based thermal management. Iterative process in ANSYS Fluent showed us that the bushbars with 2 holes of 4mm each gave us the optimal cooling condition with uniform heat distribution.

As discussed previously, the main objective of this work was to provide a first guiding step to the Formula student community especially teams who are ambitious about participating in the FSEV. Future work would consist about optimization of the mentioned steps as well as exploring ways in which such methods can be generalized so that it could serve larger purpose.

.

REFERENCES

1. M D.S. Korobkov, O.V. Ufimtseva, “Choice of the Traction Motor for the Electric Racing Car Formula Student”, Procedia Engineering, Vol 150, pp 283-288, 2016, https://doi.org/10.1016/j.proeng.2016.07.004.
2. C. Hariharan, D. Gunadevan, S. Arun Prakash, K. Latha, V. Antony Aroul Raj, R. Velraj, “Simulation of battery energy consumption in an electric car with traction and HVAC model for a given source and destination for reducing the range anxiety of the driver”, Energy, Vol 249, 2022, https://doi.org/10.1016/j.energy.2022.123657.
3. Follivi Kloutse Ayevide, Sousso Kelouwani, Ali Amamou, Mohsen Kandidayeni, Hicham Chaoui, “Estimation of a battery electric vehicle output power and remaining driving range under subfreezing conditions,” Journal of Energy Storage, Vol 55, Part B, 2022, https://doi.org/10.1016/j.est.2022.105554.
4. L. Zhao, Y. Xing, X. Liu, Experimental investigation on the thermal management performance of heat sink using low melting point alloy as phase change material, Renew. Energy, Vol 146 , pp.1578–1587, 2020, https://doi.org/10.1016/j. renene.2019.07.115.
5. Barcellona, Simone, and Luigi Piegari. "Lithium ion battery models and parameter identification techniques." Energies, Vol 10, 2017, https://doi.org/10.3390/en10122007.
6. Z. Ling, W. Lin, Z. Zhang, X. Fang, Computationally efficient thermal network model and its application in optimization of battery thermal management system with phase change materials and long-term performance assessment, Appl. Energy, Vol 259, 114120, 2020, https://doi.org/10.1016/j.apenergy.2019.114120.
7. X. Luo, Q. Guo, X. Li, et al., Experimental investigation on a novel phase change material composite coupled with graphite film used for thermal management of lithium-ion cells, Renew. Energy, Vol 145, pp. 2046–2055, 2019, https://doi.org/10.1016/ j.renene.2019.07.112.
8. Ali Ahmadian, Mahdi Sedghi, Ali Elkamel, Michael Fowler, Masoud Aliakbar Golkar, “Plug-in electric vehicle batteries degradation modeling for smart grid studies: Review, assessment and conceptual framework,” Renewable and Sustainable Energy Reviews, Vol 81, Part 2, 2018, pp. 2609-2624, https://doi.org/10.1016/j.rser.2017.06.067.
9. K. Smith, M. Earleywine, E. Wood, J. Neubauer, A. Pesaran, “Comparison of plugin hybrid electric vehicle battery life across geographies and drive cycles,” SAE Tech. Pap. 2012, https://doi.org/10.4271/2012-01-0666.
10. J. Hicks-Garner, et al., “Degradation of lithium-ion batteries employing graphite negatives and nickel–cobalt–manganese oxide + spinel manganese oxide positives: Part 1, aging mechanisms and life estimation,” J. Power Sources, Vol 269, pp. 937–948, 2014, https://doi.org/10.1016/j.jpowsour.2014.07.030.
11. R. Mathieu, I. Baghdadi, O. Briat, P. Gyan, J.M. Vinassa, “D-optimal design of experiments applied to lithium battery for ageing model calibration,” Energy Vol 141, pp. 2108–2119, 2017, https://doi.org/10.1016/j.energy.2017.11.130.
12. J. Cao, Y. He, J. Feng, S. Lin, Z. Ling, Z. Zhang, X. Fang, “Mini-channel cold plate with Nano phase change material emulsion for Li-ion battery under high-rate discharge,” Applied Energy Vol 279, 115808, 2020, https://doi.org/10.1016/j. apenergy.2020.115808.
13. H. Liu, A. Shakeel, Y. Shi, J. Zhao, “A parametric study of a hybrid battery thermal management system that couples PCM/copper foam composite with helical liquid channel cooling,” Energy, Vol 231, 120869, 2021, https://doi.org/10.1016/j. energy.2021.120869.
14. Z. Ling, W. Lin, Z. Zhang, X. Fang, “Computationally efficient thermal network model and its application in optimization of battery thermal management system with phase change materials and long-term performance assessment,” Applied Energy, Vol 259, 114120, 2020, https://doi.org/10.1016/j.apenergy.2019.114120.
15. X. Luo, Q. Guo, X. Li, et al., “Experimental investigation on a novel phase change material composites coupled with graphite film used for thermal management of lithium-ion cells,” Renewable Energy, Vol 145 pp.2046–2055, 2020, https://doi.org/10.1016/ j.renene.2019.07.112.

16. M.M. Elidi, M. Karkri, M. Abdoutankari, “A passive thermal management system of Li-ion cells using PCM composites: experimental and numerical investigations,” International Journal of Heat and Mass Transfer, Vol 169, 120894, 2021, https://doi.org/10.1016/j.ijheatmasstransfer.2020.120894.
17. P.V. Sai, B. Debangsu, “Thermal management of a high temperature sodium sulphur battery stack,” International Journal of Heat and Mass Transfer, Vol 181, 2021, https://doi.org/10.1016/j.ijheatmasstransfer.2021.122025
18. X. Mo, H. Zhi, Y. Xiao, H. Hua, L. He, “Topology optimization of cooling plates for battery thermal management,” International Journal of Heat and Mass Transfer, Vol 178, 121612, 2021, https://doi.org/10.1016/j.ijheatmasstransfer.2021.121612.